In *Proceedings of DICTA95, Digital Image Computing: Techniques and Applications*, pp. 661-666. (Conference of the Australian Pattern Recognition Society, Brisbane, Australia, 6–8 December 1995.)

NOISE REDUCTION IN SYNTHETIC APERTURE RADAR IMAGERY USING A MORPHOLOGY-BASED NONLINEAR FILTER

Mark A. Schulze and Qing X. Wu

Manaaki Whenua – Landcare Research
P O Box 38 491
Wellington Mail Centre
New Zealand

ABSTRACT

Speckle noise is a multiplicative process that is the primary source of corruption in coherently illuminated imaging modalities, including synthetic aperture radar (SAR). Theoretically, the ratio of the standard deviation to the signal value, the "coefficient of variation," is constant at every point in images corrupted by purely multiplicative noise. We introduce a new nonlinear filter based on mathematical morphology that uses this property to remove speckle noise from SAR images without blurring edges. The filter performs low-pass filtering over areas in an image where the coefficient of variation is small. Since edges and other image features usually increase the estimated coefficient of variation, the new filter smooths homogeneous regions of the image and enhances contrast at edges. Examples are given comparing the new filter to established speckle noise reduction methods on SAR images.

1. INTRODUCTION

Synthetic aperture radar (SAR) images are becoming more widely used in remote sensing applications. SAR uses microwave radiation to illuminate the earth's surface, and therefore overcomes some the problems associated with conventional visual remote sensing imagery. For example, SAR is not affected by cloud cover or variation in solar illumination. The coherent microwave illumination, however, generates a multiplicative speckle noise process that corrupts SAR images. We have used the properties of this speckle noise to develop a filtering process to reduce the noise without blurring edges or other features.

Methods used previously to reduce speckle noise in images include the local statistics method [1-4], the sigma filter [2, 3, 5, 6], the median filter, homomorphic filtering [7, 8], and adaptive linear smoothing [9, 10]. Although most of these techniques exhibit at least some degree of edge preservation, the results of these filters generally either still have too much noise or do not have distinct enough edges to allow simple edge detection algorithms to perform well. We have developed a new nonlinear filter that uses local measurements of the noise in the image to guide a low-pass filtering operation to act only over regions where the original signal is estimated to be homogeneous. Speckle is therefore reduced in these areas but the edges between them remain intact. This filter uses a new filtering structure [11] based on mathematical morphology and is effective enough at reducing noise and sharpening edges that even simple edge detection algorithms return good edge maps from the filtered images.

2. SPECKLE NOISE MODEL

The speckle noise of SAR images is usually modeled as purely multiplicative noise process of the form given in equation (2.1) below. For SAR, the noise n is assumed to have a mean value $\bar{n} = 1$. The pixel values returned by the radar imaging process (g) are the product of the true radiometric values f and the speckle noise n.

$$g = f \cdot n \tag{2.1}$$

The statistics of the speckle noise are well-known [3, 12, 13]. Single-look SAR amplitude images have Rayleigh-distributed noise, and single-look intensity images have negative exponentially distributed noise. Multi-look SAR images have gamma-distributed noise, assuming that the looks are independent.

3. FILTERING ALGORITHM

3.1. Value-and-criterion filter structure

The value-and-criterion filter structure [11] is a new framework for designing filters based on mathematical morphology. Whereas morphological filters use only nonlinear (minimum and maximum) operators, the value-and-criterion structure allows both linear and nonlinear operators. However, the new filtering structure retains the strong geometrical component of morphological filters. The value-and-criterion filter structure, therefore, exhibits the shape-based characteristics of mathematical morphology but adds a great deal of flexibility in the selection of filtering operations.

A value-and-criterion filter is a two-stage operation similar to the morphological opening and closing operators. Opening performs a morphological erosion (a sliding minimum operation) followed by a morphological dilation (a sliding maximum operation). Similarly, closing is dilation followed by erosion. Like opening and closing, the output of a value-and-criterion filter results from the second-stage operator that acts on the output of the first stage of the filter. Unlike the morphological operators, however, the first stage of a value-and-criterion filter consists of two separate operations, a *criterion* operator and a *value* operator. The second stage of the filter uses the results of the criterion operator to choose an output of the value operator for the final output. This new filter structure unites many different types of nonlinear filters into a single mathematical formalism.

The "value" function, V, and the "criterion" function, C, act on the original image $\mathbf{g}(x)$ and are defined over a structuring element (filter window) N. The "selection" operator, S, comprises the second stage of the filter and acts on the output of the criterion function. As in morphological filters, the second stage (S) is defined over the structuring element $\tilde{N}$, a 180° rotation of N. Let $g(\mathbf{x})$ be the input to a value-and-criterion filter, and $v(\mathbf{x})$, $c(\mathbf{x})$, and $s(\mathbf{x})$ be the output of V, C, and S respectively. The filter output $f(\mathbf{x})$ is defined by equations (3.1)–(3.4) below [11].

$$v(\mathbf{x}) = V\{g(\mathbf{x}); N\} \tag{3.1}$$

$$c(\mathbf{x}) = C\{g(\mathbf{x}); N\} \tag{3.2}$$

$$s(\mathbf{x}) = S\{c(\mathbf{x}); \tilde{N}\} \tag{3.3}$$

$$\hat{f}(\mathbf{x}) = v\left(\left\{\mathbf{x}' : \mathbf{x}' \in \tilde{N}_{\mathbf{x}};\ c(\mathbf{x}') = s(\mathbf{x})\right\}\right) \tag{3.4}$$

$\tilde{N}_{\mathbf{x}}$ denotes the translation of $\tilde{N}$ such that it is centred at position $\mathbf{x}$.

The value-and-criterion structure is a superset of the morphological opening and closing operators. Morphological opening results when V and C are both the minimum operator and S is the maximum operator, and closing results when V and C are the maximum operator and S is the minimum operator. Designing new nonlinear filters with the value-and-criterion structure is simply a matter of choosing different V and C functions.

The value-and-criterion filter structure has the same comprehensive "subwindow" structure that develops naturally in morphological opening and closing. This structure is more comprehensive than those of previous subwindow-based filtering schemes [14-16]. The value-and-criterion filter structure with an $n \times n$ square structuring element develops an overall filtering window of size $(2n\text{-}1) \times (2n\text{-}1)$ that contains n^2 "subwindows" the same size and shape as the structuring element. These subwindows are all the possible $n \times n$ structuring elements that fit in the overall

window. Within each overall window, the structuring element that yields the "selected" criterion function value is chosen, and the value function output from that structuring element becomes the filter output for the overall window. The operation of this filter structure is very efficient, since the value and criterion function outputs for each subwindow are only computed once per image, unlike many of the earlier related filters.

3.2. Minimum Coefficient of Variation (MCV) filter

We have used the value-and-criterion filter structure to design the Minimum Coefficient of Variation (MCV) filter to reduce speckle noise in SAR images without blurring or distorting edges. The idea behind the MCV filter is to direct a low-pass filtering operation (the value function) to act only in areas that do not contain edges by choosing appropriate criterion and selection functions. The MCV filter uses the sample mean as its value function (low-pass filter) and performs this filtering over areas with the smallest estimated coefficient of variation.

Local estimates of the coefficient of variation in an image are found by computing the ratio of the sample standard deviation and sample mean within a structuring element. These estimates are close to the expected theoretical value of the coefficient in regions where the signal is constant in the structuring element. In areas where the signal is not constant because of edges or other features, estimates of the coefficient are higher than the expected value. Selecting the structuring element with the minimum coefficient of variation therefore directs the MCV filter to smooth only over regions without prominent edges or other features.

The MCV filter, therefore, has V = sample mean, C = sample coefficient of variation, and S = minimum. At every point in an image, this filter effectively selects the $n \times n$ subwindow within an overall window of $(2n\text{-}1) \times (2n\text{-}1)$ that has the smallest measured coefficient of variation, and outputs the mean of that subwindow. Since subwindows which include edges or other features have a higher measured coefficient of variation than uniform subwindows, the average is taken over areas that do not contain edges. By flattening regions near gradual edges, the MCV filter not only preserves but also enhances edges.

4. EXAMPLES

4.1. Previous SAR speckle reduction methods

Many techniques have been used to reduce speckle in images. Common techniques include the local statistics method [1-4], the sigma filter [2, 3, 5, 6], the median filter, homomorphic filtering [7, 8], and adaptive linear smoothing [9, 10]. Durand *et al.* [4] compared 10 different filtering methods for speckle reduction in SAR images and found that a modified version of the local statistics method, given in equation (4.1) below, performed best. The input image (corrupted by speckle noise) is g, the filter output is $\hat{f}$, the local mean and standard deviation of g are given by $\bar{g}$ and σ_g, respectively, and the standard deviation of the speckle noise is σ_n. The value of σ_n is theoretically a known constant for a given image; for a 3-look SAR intensity image with independent looks, $\sigma_n = 0.2941$ (see Lee [3]).

$$\hat{f} = \bar{g} + (g - \bar{g}) \cdot \frac{\left(1 - \bar{g}^2 \cdot \frac{\sigma_n^2}{\sigma_g^2}\right)}{\left(1 + \sigma_n^2\right)} \tag{4.1}$$

4.2. Filter comparison on phantom image with simulated 3-look speckle noise

To compare the MCV filter with earlier SAR filtering techniques, we have developed a phantom image with several different ellipsoidal and rectangular features. We have simulated 3-look speckle noise in the image using the multiplicative noise model of Section 2. The various filters

have been applied and the mean absolute error (MAE) and mean square error (MSE) between the filtered images and the known original image computed. A small subimage (88×64 pixels) of the phantom image is shown in Figure 1, along with the noisy and filtered versions. The MCV filter is the most effective of the filters at reducing the speckle noise. Table 1 gives values for the MAE and MSE between the filtered images and original image; note that these values are lowest for the 5×5 MCV filters. The two MCV filters shown have different structuring element shapes; the "square" MCV filters have simple square structuring elements, while the "round" MCV filters have structuring elements approximating a circle. For a size 5×5 structuring element, the "round" shape is equivalent to a 5×5 square with the four corner pixels removed.

Table 1. MAE and MSE for various SAR noise reduction algorithms for a phantom image corrupted by simulated 3-look speckle noise.

Algorithm	Window Size	MAE	MSE
(unprocessed)	—	10.38	290.2
local statistics method (Lee)	5×5	6.51	128.4
	7×7	6.59	132.7
local statistics method (Durand)	5×5	5.50	92.1
	7×7	5.39	89.9
MCV filter (square)	5×5	4.43	66.6
	7×7	4.94	87.2
MCV filter (round)	5×5	4.32	59.2
	7×7	4.61	71.1

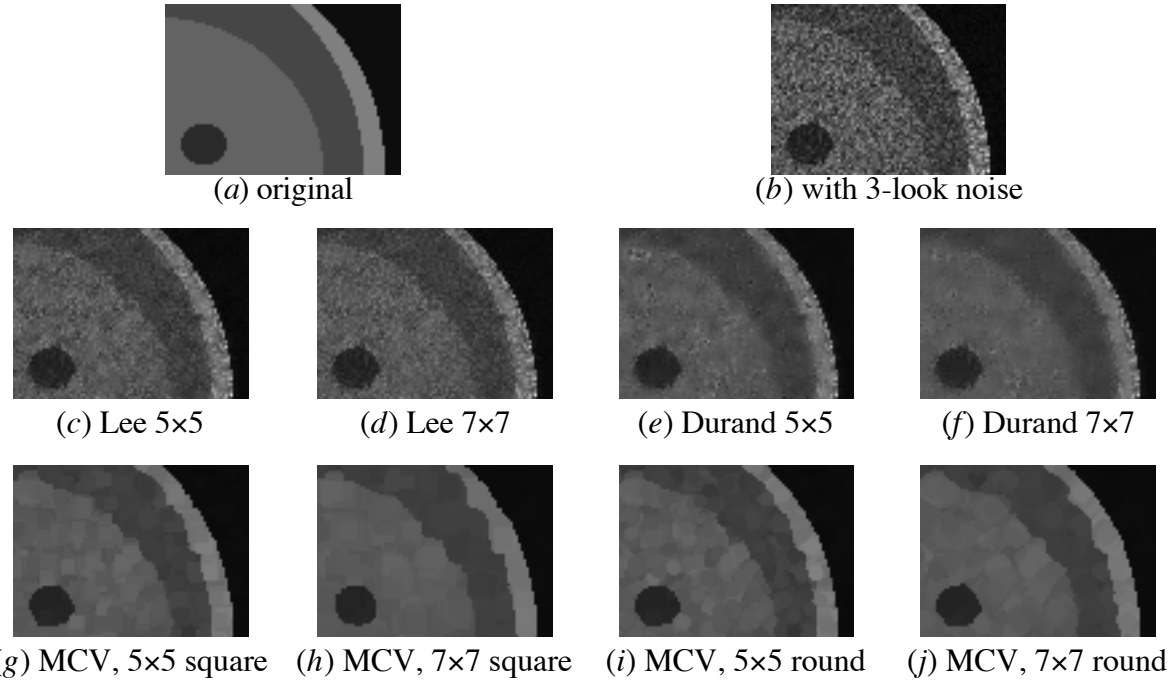

(*a*) original (*b*) with 3-look noise

(*c*) Lee 5×5 (*d*) Lee 7×7 (*e*) Durand 5×5 (*f*) Durand 7×7

(*g*) MCV, 5×5 square (*h*) MCV, 7×7 square (*i*) MCV, 5×5 round (*j*) MCV, 7×7 round

Figure 1. Portion of phantom image with simulated 3-look SAR noise filtered by Lee's local statistics method [1], the modified method of Durand [4], and the MCV filter with square and round structuring elements.

4.3. Filter comparison on a SAR image

Figures 2–5 below illustrate the effect of MCV filtering compared to the local statistics filtering method on a SAR image taken by the JERS-1 satellite of a peninsula extending into Port Underwood in the Marlborough Sounds of New Zealand. JERS-1 images are 3-look SAR images that closely obey the noise model of Section 2 [17]. The MCV-filtered images (Figures 4 and 5) have sharper edges and less prominent noise than the local statistics filtered image

(Figure 3). Figures 6–9 show the results of applying the Canny edge detection algorithm [18] to the images in Figures 2–5, followed by thresholding at a constant level. The edges detected from the MCV-filtered images are much clearer and there are far fewer false edges than in the local statistics filtered image.

5. CONCLUSIONS

The Minimum Coefficient of Variation (MCV) filter is a new nonlinear filter based on mathematical morphology that we have designed to reduce speckle noise in SAR images without blurring edges. The MCV filter takes into account the speckle noise model for SAR images and outperforms existing filtering methods on both simulated and real radar images.

6. REFERENCES

1. J.-S. Lee (1981). "Speckle analysis and smoothing of synthetic aperture radar images." *Computer Graphics and Image Processing*, v. 17 n. , pp. 24-32.
2. J.-S. Lee (1983). "A simple speckle smoothing algorithm for synthetic aperture radar images." *IEEE Transactions on Systems, Man, and Cybernetics*, v. 13 n. 1, pp. 85-89.
3. J.-S. Lee (1986). "Speckle suppression and analysis for synthetic aperture radar images." *Optical Engineering*, v. 25 n. 5, pp. 636-643.
4. J.M. Durand, B.J. Gimonet *et al.* (1987). "SAR data filtering for classification." *IEEE Transactions on Geoscience and Remote Sensing*, v. 25 n. 5, pp. 629-637.
5. J.-S. Lee (1983). "Digital image smoothing and the sigma filter." *Computer Vision, Graphics, and Image Processing*, v. 24 n. 2, pp. 255-269.
6. J.-S. Lee and I. Jurkevich (1990). "Coastline detection and tracing in SAR images." *IEEE Transactions on Geoscience and Remote Sensing*, v. 28 n. 4, pp. 662-668.
7. G. Franceschetti, V. Pascazio *et al.* (1995). "Iterative homomorphic technique for speckle reduction in synthetic-aperture radar imaging." *Journal of the Optical Society of America A*, v. 12 n. 4, pp. 686-694.
8. H.H. Arsenault and M. Levesque (1984). "Combined homomorphic and local-statistics processing for restoration of images degraded by signal-dependent noise." *Applied Optics*, v. 23 n. 6, pp. 845-850.
9. V.S. Frost, J.A. Stiles *et al.* (1981). "An adaptive filter for smoothing noisy radar images." *Proceedings of the IEEE*, v. 69 n. 1, pp. 133-135.
10. V.S. Frost, J.A. Stiles *et al.* (1982). "A model for radar images and its application to adaptive digital filtering for multiplicative noise." *IEEE Transactions on Pattern Analysis and Machine Intelligence*, v. 4 n. 2, pp. 157-165.
11. M.A. Schulze and J.A. Pearce (1994). "A morphology-based filter structure for edge-enhancing smoothing." *1994 IEEE International Conference on Image Processing (ICIP-94)*, Austin, Texas, pp. 530-534.
12. L.J. Porcello, N.G. Massey *et al.* (1976). "Speckle reduction in synthetic-aperture radars." *Journal of the Optical Society of America*, v. 66 n. 11, pp. 1305-1311.
13. G.V. April and E.R. Harvey (1991). "Speckle statistics in four-look synthetic aperture radar imagery." *Optical Engineering*, v. 30 n. 4, pp. 375-381.
14. M. Kuwahara, K. Hachimura *et al.* (1976). "Processing of RI-angiocardiographic images." In *Digital Processing of Biomedical Images*, K. Preston Jr. and M. Onoe, eds. New York: Plenum, pp. 187-202.
15. M. Nagao and T. Matsuyama (1979). "Edge preserving smoothing." *Computer Graphics and Image Processing*, v. 9 n. , pp. 394-407.
16. J.-S. Lee (1980). "Digital image enhancement and noise filtering by use of local statistics." *IEEE Transactions on Pattern Analysis and Machine Intelligence*, v. 2 n. 2, pp. 165-168.
17. Q.X. Wu and M.A. Schulze (1995). "Statistical properties of three-look JERS-1 SAR data." *Image and Vision Computing in New Zealand Workshop 1995 (IVCNZ95)*, Christchurch, New Zealand, pp. 197-202.
18. J. Canny (1986). "A computational approach to edge detection." *IEEE Transactions on Pattern Analysis and Machine Intelligence*, v. 8 n. 6, pp. 679-698.

Figure 2. Original SAR image of Port Underwood, New Zealand.

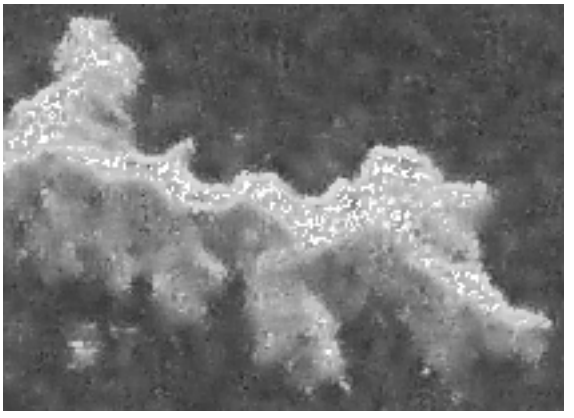

Figure 3. Image filtered by the local statistics method (Durand), size 7×7.

Figure 4. Square MCV filtering (5×5).

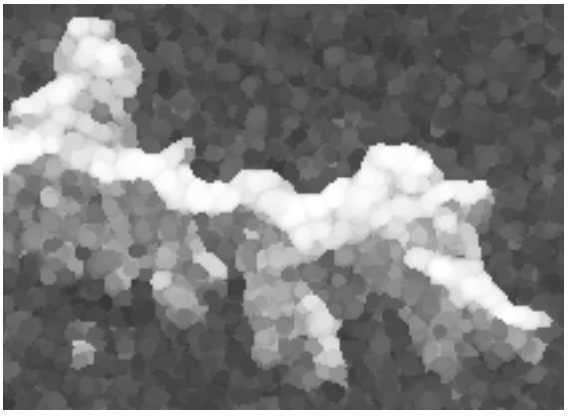

Figure 5. Round MCV filtering (5×5).

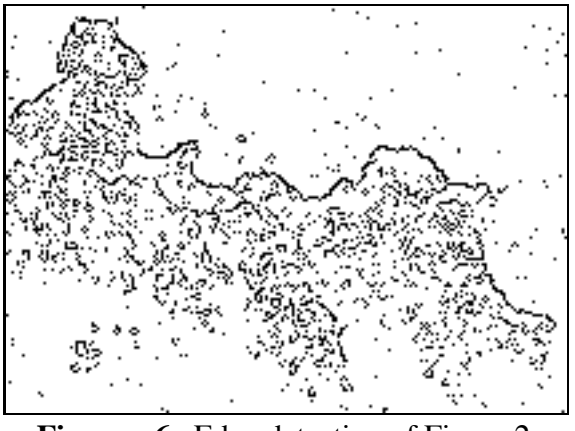

Figure 6. Edge detection of Figure 2.

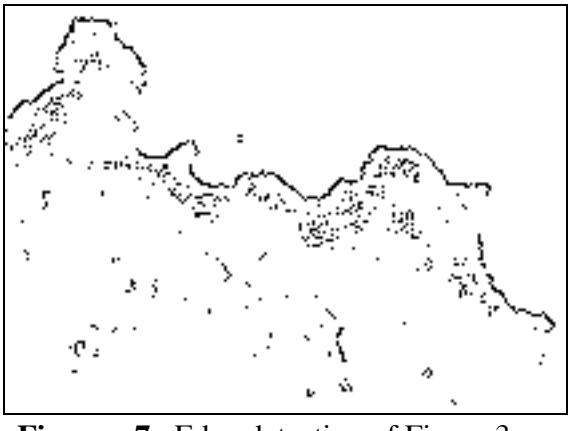

Figure 7. Edge detection of Figure 3.

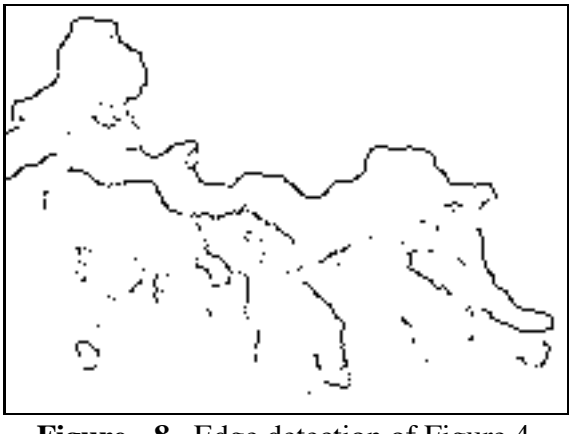

Figure 8. Edge detection of Figure 4.

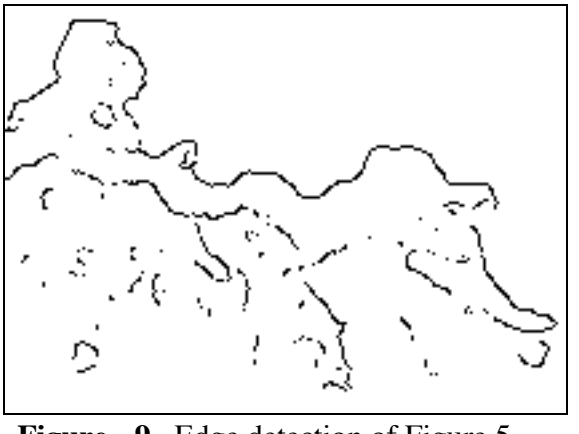

Figure 9. Edge detection of Figure 5.